

Power Generation and Anode Bacterial Community Compositions of Sediment Fuel Cells Differing in Anode Materials and Carbon Sources

Sokhee P. Jung^{1,*}, Mi-Hwa Yoon², Seung-Mok Lee^{2,*}, Sang-Eun Oh³, Hojeong Kang¹, Jae-Kyu Yang⁴

¹School of Civil and Environmental Engineering, Yonsei University, Seoul, Republic of Korea

²Department of Environmental Engineering, Kwandong University, Gangneung, Republic of Korea

³Department of Biological Environment, Kangwon National University, Chuncheon, Republic of Korea

⁴Division of General Education, Kwangwoon University, Seoul, Republic of Korea

*E-mail: sokheejung@gmail.com; slee@kwandong.ac.kr

Received: 23 September 2013 / Accepted: 31 October 2013 / Published: 15 November 2013

For monitoring environmental conditions of remote places, sustainable power generators are necessary to power telemetry sensor systems. A sediment microbial fuel cell (SMFC) is a device that produces electricity biologically from organic matters in sediment. Because a SMFC utilizes sediment organic materials and microbial catalysts in river or oceanic sediment, a SMFC can be a feasible solution for sustainable power generation in remote places. However, oligotrophic sediment conditions often limit energy source supply, resulting in insufficient power output for operating electronic devices. The objective of this study is to investigate power generation and anode bacterial communities of SMFCs with different anode materials and carbon sources for enhancement of power output and longevity of SMFCs. Four kinds of anode electrodes were tested in SMFCs; a magnesium electrode (M), a magnesium electrode supplied with chitin particles (M+C), a graphite electrode (G), and a graphite electrode supplied with chitin particles (G+C). Average maximum power density was highest in Mg+C ($1878 \pm 982 \text{ mW m}^{-2}$), followed by M ($848 \pm 348 \text{ mW m}^{-2}$), G+C ($1.9 \pm 0.6 \text{ mW m}^{-2}$) and G ($0.7 \pm 0.6 \text{ mW m}^{-2}$). Maximum power densities of the magnesium electrodes were ~1,000 times larger than those of the graphite electrodes. The chitin supplement increased maximum power densities by 121% in the magnesium anodes and 164% in the graphite anodes on average. A magnesium electrode in M+C degraded more slowly than that of M. Anode bacterial communities of the magnesium anodes were diverse than the graphite anodes, and the supplemented chitin greatly influenced anode bacterial community compositions. Although magnesium corrosion was a main process of power production in the magnesium-anode SMFCs, species-level anode bacterial communities were very different between M and M+C. Anode bacterial communities of the chitin-absent anodes had larger richness estimates and diversity estimates than those of the chitin-supplemented anodes, suggesting that the saturated carbon source greatly simplified anode bacterial communities.

Keywords: Sediment MFC, pyrosequencing, anode microbial community, chitin, magnesium electrode

1. INTRODUCTION

For monitoring environmental conditions of remote places, sustainable power generators are necessary to power sensors and telemetry systems because replacing batteries there can be costly and time-consuming in many situations. A sediment microbial fuel cell (SMFC) can be a feasible solution for this purpose. A SMFC is a device that can directly produce electricity from the bacterial oxidation of organic sediment in remote places [1-6]. SMFCs typically consist of conductive anode such as a graphite embedded in an anaerobic sediment and a catalyst-coated cathode made of a graphite plate or carbon fibers suspended in the overlying oxygenated water (Fig. 1A).

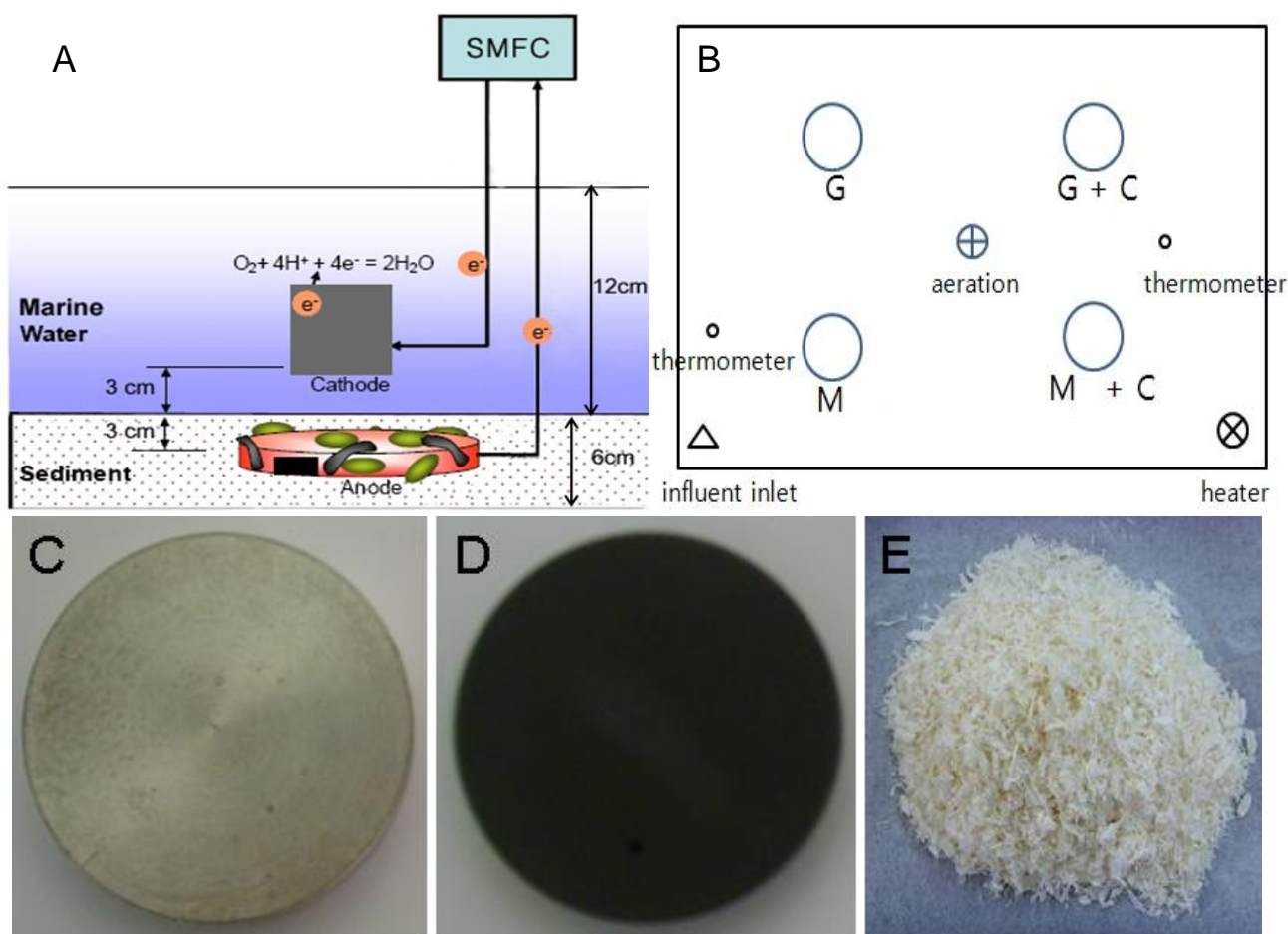


Figure 1. Schematic diagrams of the SMFC setting (A-a side view; B-a top view), magnesium anode (C), graphite anode (D) and chitin powders (E) [7]

However, because natural sediment conditions often provide limited amount of organic matter, low power output is generated from SMFCs in these conditions. The initial type of SMFCs produced a stable power density of 10 - 20 mW m⁻² in the marine sediment containing 2-6% of organic matter [1,

2]. Because typical sediments contain 0.4 - 2.2% of organic matter contents [4], power density could be enhanced in sediments with higher organic contents [1]. So, particulate chitin and cellulose powder were added to anode electrodes to increase power output from SMFCs [4]. Maximum power densities were $\sim 80 \text{ mW m}^{-2}$ in the both cases with $\sim 2 \text{ mW m}^{-2}$ for a control. Although power densities of SMFC increased significantly by adding the particulate substrates, the levels of power were still insufficient for powering commercial electronics. For this reason, a sacrificial anode made of magnesium alloy was applied in the MFC system, which was able to produce a maximum of 2.1 V [8, 9].

To identify core exoelectrogens and understand the anode exoelectrogenic reactions, anode bacterial communities of SMFCs were analyzed in various sediment conditions [2, 10]. Anode bacterial communities have been classified as iron reducing bacteria affiliated with the *Geobacteraceae* family [2]. *Desulfurumonas* spp. were dominant in anode microbial community in marine sediments, while the *Geobacter* spp. were in freshwater sediments [10]. However, anode microbial communities of magnesium electrodes have not yet been characterized. Anode biofilm is a crucial component in bioelectricity production, and it is important to understand the bioanode process better for power enhancement by analyzing microbial communities and electrochemistry [11-15]. In this study, four SMFCs were constructed by using a magnesium anode or a graphite anode and chitin powers were applied. Voltage and power densities of the SMFCs were monitored during the 40 day operation and their anode bacterial communities were investigated for a better understanding of the bioanode process.

2. MATERIALS AND METHODS

2.1. Construction of anode and cathode electrodes

Titanium wires (5 cm diameter and 1 cm thickness) were used to connect SMFC circuits. Conductive epoxy was applied to create low-resistance connections between electrodes and wires. And non-conductive epoxy was applied to protect the electrical connections from water. Overall, four kinds of anode electrodes were tested; a magnesium electrode (M), a magnesium electrode supplied with 1 g of chitin (M+C), a graphite electrode (G), and a graphite electrode supplied with 1 g of chitin (G+C). The cathodes were made by applying platinum (0.5 mg/cm^2 Pt) and four diffusion layers on non-wet-proofed carbon cloth (type A, E-TEK) as previously described [16].

2.2. SMFC chamber construction and operation

Laboratory scale aquatic chamber (450 mm \times 300 mm \times 340 mm) was filled with marine sediment taken from East Sea in Korea (Fig. 1A). The four anodes were installed on 3 cm above from the bottom of the chamber, and the anodes were covered with marine sediment of 6-cm thickness. Artificial seawater (Tetra Marine Salt, United Pet Group Inc, USA) was used to mimic the marine sediment condition. The chamber was filled with the artificial seawater containing 33 g/L of sea salt up to 12-cm water level. Anode and cathode wires were connected with voltage-current measurement device (Kynel, Korea). Open circuit voltage (OCV) was measured for the first two days and then

closed circuit voltages were measured with different resistances. The artificial seawater was periodically replenished to maintain water level. Temperature of the chamber was maintained at 30 °C and an aeration rate was 6 ml s⁻¹.

2.3. DNA extraction, PCR and pyrosequencing

Surfaces of the anode electrodes were scraped by using spatula for DNA extractions. Scraped anode debris, closely adjacent sediment and degraded chitin were used for DNA extraction by using FastDNA Spin Kit for Soil according to the manufacture manual (MP BIO, Cat. No. 6560-200). Integrity of genomic DNA was confirmed using gel electrophoresis. DNAs were diluted to equilibrate concentrations and purified using UltraClean DNA purification kit (Mo-bio, Cat No. 12100-300) before PCR amplification. Purified DNAs were amplified by targeting V1 - V3 regions of bacterial 16S rRNA gene (~450 bp based on *E. coli* genome) using the primer set of forward primer V1-9F (5'-CCTATCCCCTGTGTGCCTTGGCAGTC-TCAG-AC-GAGTTTGATCMTGGCTCAG-3') and reverse primer V3-541R (5'-CCATCTCATCCCTGCGTGTCTCCGAC-TCAG-X-AC-WTTACCGCGGCTGCTGG-3'). The first two primer sections are adaptor and key, AC is a linker and underlined sequences are gene specific primers. X in the reverse primer is a barcode primer. PCR amplification was performed in a 50 ul-volume containing 1.25U Taq DNA Polymerase, 5 µl 10 × PCR reaction buffer, 0.2 mM dNTP mix, 0.4 µM of each primer, and of 1 µ of template DNA (Roche Cat. No. 04-728-882-001) with the following thermalcycler program: initial denaturation at 95 °C for 5 min; 30 cycles of denaturation at 95 °C for 30 s, annealing at 55 °C for 30 s, and extension at 72°C for 60 s; and a final extension at 72°C for 7 min in PTC-200 DNA Engine (MJ Research, MN). Size and contamination of PCR amplicons were confirmed by gel electrophoresis. Quality of PCR products was confirmed by gel electrophoresis. PCR products were purified using QIAquick PCR Purification Kit (QIAGEN, Cat. No. 28106) and several reactions were pooled in a 1.5-ml tube. Bands shorter than 300 bp were removed using QIAquick Gel Extraction Kit (QIAGEN, Cat. No. 28706) in a following gel electrophoresis. 1 µg of PCR product was subjected to pyrosequencing. The Pyrosequencing was performed with 454 GS FLX Titanium (454 Life Science, Rosche) in Chunlab, Inc. (Seoul, Korea) according to the manufacturer's instructions.

2.4. Analysis of pyrosequencing data

DNA sequences from each sample were separated by unique barcodes. Barcodes, linkers, and gene-specific primers were removed from original sequencing reads after pyrosequencing. Samples were filtered to select the DNA sequences above 300 base pairs. Nonspecific sequences (expectation value of $>e^{-5}$) in a BLASTN search and chimeric sequences were removed. For the taxonomic assignment of each pyrosequencing read, EzTaxon-e database (<http://www.eztaxon-e.org>) was used [17]. Operational taxonomic units (OTUs) were defined at the 3% divergence threshold using the average neighbor clustering algorithm. CD-HIT was used for massive clustering of metagenomic sequences [18], and corresponding graphical representations were generated using CLcommunity 3.0

(Chunlab Inc., Seoul, Korea). Abundance-based coverage estimator (ACE), Chao 1 estimator (Chao), interpolated Jackknife richness estimator (Jack), non-parametric Shannon diversity index (NpShannon), Shannon index of diversity (Shannon), Simpson index of diversity (Simpson) and Good's coverage were calculated using Mothur 1.28.0 [19].

Table 1. Time-course maximum power densities (P_{\max}) produced from each SMFC with a magnesium anode, a magnesium anode with the chitin, a graphite anode, or a graphite anode with the chitin [7]. Maximum power density is calculated by dividing power by 200 cm^2 of the cathode area

Time (hr)	$P_{\max}(\text{mW}/\text{m}^2)$			
	Mg	Mg+C	G	G+C
72	1099.0	1575.0	0.0	1.8
168	392.0	3328.0	0.5	2.7
312	1140.0	1162.0	1.3	1.8
408	762.0	1445.0	1.1	1.4
Average	848.3	1877.5	0.7	1.9
Stdev	348.1	982.3	0.6	0.6

3. RESULTS AND DISCUSSION

3.1. Electrochemical Performance

The SMFCs (M, M+C, G and G+C) were operated in open circuit mode for the initial 50 hours, and were operated in closed circuit mode during the remaining 800 hour operation. Open-circuit voltages were $\sim 1.8 - 2.3 \text{ V}$ in M, $\sim 1.6 - 2.5 \text{ V}$ in M+C, $\sim 0.6 - 0.8 \text{ V}$ in G and $\sim 0.6 - 0.8 \text{ V}$ in G+C. Closed-circuit voltages at a $1000\text{-}\Omega$ external resistor were $\sim 1.2 - 1.8 \text{ V}$ in M+C, $\sim 0 - 1.8 \text{ V}$ in M, $\sim 0.3 - 0.4 \text{ V}$ in G and $0.1 - 0.3 \text{ V}$ in G+C. Cell voltages were higher in the magnesium anodes (M and M+C) than the graphite anodes (G and G+C) as suggested by standard reduction potential of magnesium, glucose and acetate (Mg^{2+}/Mg , $E^\circ = -2.37 \text{ V}$; $\text{CO}_2/\text{glucose}$, $E^\circ = -0.43 \text{ V}$; $\text{CO}_2/\text{acetate}$, $E^\circ = -0.28 \text{ V}$) [20]. The chitin-supplemented anodes (M+C and G+C) had slightly higher cell voltages than the chitin-absent anodes (M and G) in each anode material. Closed-circuit voltages in M decreased sharply from 300 hours and became 0 after the 650 hour operation because degradation of the magnesium electrode made the electrical circuit disconnected. A magnesium electrode in M+C degraded more slowly than that of M possibly because chitin particles might slow down the magnesium corrosion in

M+C. Addition of chitin particles was demonstrated to enhance voltage and longevity of SMFCs in a previous study [4]. Closed-circuit voltages of M+C decreased consistently in the beginning and maintained ~1.2 V thereafter. Closed-circuit voltages of the graphite anodes were relatively constant over the entire operation in a closed circuit mode.

Maximum power densities of SMFCs were measured four times. Maximum power densities were highly variable in each measurement. Average maximum power density was highest in Mg+C ($1878 \pm 982 \text{ mW m}^{-2}$), followed by M ($848 \pm 348 \text{ mW m}^{-2}$), G+C ($1.9 \pm 0.6 \text{ mW m}^{-2}$) and G ($0.7 \pm 0.6 \text{ mW m}^{-2}$) (Table 1). Maximum power densities of the magnesium electrodes were ~1,000 times larger than those of the graphite electrodes. Because the only substrate was sediment organic compounds in the SMFC with G, the chitin supplement increased power output in the oligotrophic sediment condition. The chitin supplement increased average maximum power densities by 121% in the magnesium anodes (M+C vs. M) and 164% in the graphite anodes (G+C vs. G) (Table 1).

Table 2. The five most dominant compositions of anode bacterial communities at 436 sequence reads (uc: unclassified)

Rank	Phylum	M(%)	Phylum	M+C(%)
1	<i>Proteobacteria</i>	56.1	<i>Firmicutes</i>	51.6
2	<i>Firmicutes</i>	34.2	<i>Proteobacteria</i>	47.7
3	<i>Bacteroidetes</i>	2.8	<i>Actinobacteria</i>	0.5
4	<i>Actinobacteria</i>	2.9	<i>Cyanobacteria</i>	0.2
5	<i>Chloroflexi</i>	2.2	<i>Chloroflexi</i>	0.0
Sum		98.2		100.0
Rank	Class	M(%)	Class	M+C(%)
1	<i>Deltaproteobacteria</i>	34.8	<i>Bacilli</i>	51.6
2	<i>Bacilli</i>	18.8	<i>Alphaproteobacteria</i>	47.2
3	<i>Clostridia</i>	15.4	<i>Gammaproteobacteria</i>	0.5
4	<i>Gammaproteobacteria</i>	12.1	<i>Actinobacteria</i>	0.5
5	<i>Alphaproteobacteria</i>	5.5	<i>Chroobacteria</i>	0.2
Sum		86.5		100.0
Rank	Order	M(%)	Order	M+C(%)
1	<i>Bacillales</i>	18.5	<i>Bacillales</i>	51.6
2	<i>Desulfuromonadales</i>	17.7	<i>Rhizobiales</i>	42.7
3	<i>Clostridiales</i>	15.2	<i>Sphingomonadales</i>	4.6
4	<i>Desulfovibrionales</i>	10.9	<i>Micrococcales</i>	0.5
5	<i>Desulfobacterales</i>	5.6	<i>Thiotrichales</i>	0.2
Sum		67.9		99.5

Rank	Family	M(%)	Family	M+C(%)
1	<i>Staphylococcaceae</i>	17.1	<i>Bacillaceae</i>	51.6
2	<i>Desulfuromonadaceae</i>	17.4	<i>Bradyrhizobiaceae</i>	41.3
3	<i>Desulfomicrobiaceae</i>	10.6	<i>Sphingomonadaceae</i>	4.6
4	<i>Desulfobacteraceae</i>	5.4	<i>Methylobacteriaceae</i>	1.1
5	<i>Enterobacteriaceae</i>	5.0	<i>Microbacteriaceae</i>	0.5
Sum		55.4		99.1
Rank	Genus	M(%)	Genus	M+C(%)
1	<i>Staphylococcus</i>	17.0	<i>Bacillus</i>	51.1
2	<i>Desulfuromusa</i>	16.8	<i>Afipia</i>	28.2
3	<i>Desulfomicrobium</i>	10.2	<i>Bradyrhizobium</i>	12.4
4	<i>Desulfobotulus</i>	4.7	<i>Sphingomonas</i>	3.4
5	<i>Escherichia</i>	4.6	<i>Bosea</i>	1.1
Sum		53.4		96.33
Rank	Species	M(%)	Species	M+C(%)
1	EU531777 (<i>Desulfuromusa</i>)	16.4	<i>Afipia birgiae</i>	27.3
2	<i>Staphylococcus xylosum</i>	15.1	<i>Bacillus subtilis</i>	22.7
3	<i>Desulfomicrobium baculatum</i>	10.1	<i>Bradyrhizobium japonicum</i>	11.2
4	<i>Desulfobotulus alkaliphilus</i>	4.7	<i>Bacillus mojavenensis</i>	10.8
5	<i>Escherichia coli</i>	4.5	<i>Bacillus siamensis</i>	9.2
Sum		50.9		81.2
Rank	Phylum	G(%)	Phylum	G+C(%)
1	<i>Proteobacteria</i>	85.6	<i>Proteobacteria</i>	96.3
2	<i>Firmicutes</i>	5.0	<i>Firmicutes</i>	1.4
3	<i>Chloroflexi</i>	3.7	<i>Spirochaetes</i>	0.7
4	<i>Bacteroidetes</i>	2.3	<i>Lentisphaerae</i>	0.4
5	<i>Spirochaetes</i>	0.8	<i>Chloroflexi</i>	0.4
Sum		97.5		99.1
Rank	Class	G(%)	Class	G+C(%)
1	<i>Deltaproteobacteria</i>	83.5	<i>Deltaproteobacteria</i>	95.9
2	<i>Bacilli</i>	4.5	<i>Bacilli</i>	1.1
3	<i>Anaerolineae</i>	3.6	<i>Spirochaetes</i>	0.7
4	<i>Bacteroidia</i>	2.0	<i>Clostridia</i>	0.2
5	<i>Gammaproteobacteria</i>	1.1	<i>Alphaproteobacteria</i>	0.2

Sum		94.6		98.2
Rank	Order	G(%)	Order	G+C(%)
1	AB015588_uc(<i>Deltaproteobacteria</i>)	66.7	<i>Desulfuromonadales</i>	95.2
2	<i>Desulfobacterales</i>	14.8	<i>Bacillales</i>	1.1
3	<i>Anaerolinaeles</i>	3.5	<i>Spirochaetales</i>	0.7
4	<i>Bacillales</i>	4.3	<i>Desulfovibrionales</i>	0.4
5	<i>Bacteroidales</i>	2.0	AJ431234 (<i>Lentisphaera</i>)	0.2
Sum		91.3		97.6
Rank	Family	G(%)	Family	G+C(%)
1	AB015588_uc(<i>Deltaproteobacteria</i>)	48.3	<i>Desulfuromonadaceae</i>	95.1
2	EU287221_uc(<i>Deltaproteobacteria</i>)	16.4	<i>Staphylococcaceae</i>	1.1
3	<i>Desulfobulbaceae</i>	11.6	<i>Spirochaetaceae</i>	0.7
4	<i>Staphylococcaceae</i>	4.1	<i>Deltaproteobacteria_uc</i>	0.2
5	<i>Anaerolinaceae</i>	3.1	<i>Desulfovibrionaceae</i>	0.3
Sum		83.6		97.3
Rank	Genus	G(%)	Genus	G+C(%)
1	AB015588_uc(<i>Deltaproteobacteria</i>)	48.3	<i>Desulfuromonas</i>	90.7
2	EU287221_uc(<i>Deltaproteobacteria</i>)	16.1	<i>Desulfuromusa</i>	1.5
3	AF420336_uc(<i>Desulfobulbaceae</i>)	8.6	<i>Desulfuromonadaceae_uc</i>	1.9
4	<i>Staphylococcus</i>	4.1	<i>Staphylococcus</i>	1.0
5	<i>Desulfocapsa</i>	2.8	<i>Pelobacter</i>	0.4
Sum		79.9		95.6
Rank	Species	G(%)	Species	G+C(%)
1	AB015588_uc(<i>Deltaproteobacteria</i>)	48.3	<i>Desulfuromonas acetoxidans</i>	76.9
2	EU287221_uc(<i>Deltaproteobacteria</i>)	16.1	<i>Desulfuromonas_uc</i>	13.5
3	AF420336_uc(<i>Desulfobulbaceae</i>)	8.5	<i>Desulfuromonadaceae_uc</i>	1.9
4	<i>Staphylococcus xylosus</i>	3.8	<i>Desulfuromusa succinoxidans</i>	0.7
5	<i>Desulfocapsa sulfexigens</i>	2.3	<i>Staphylococcus xylosus</i>	1.0
Sum		79.0		94.0

3.2. Pyrosequencing analyses of anode bacterial communities

Pyrosequencing analyses targeting the V1-V3 region of the 16S rRNA genes recovered 2,245 reads in M (average length 463 bp), 450 reads in M+C (average length 438 bp), 9,730 reads in G

(average length 472 bp) and 2,339 reads in G+C (average length 460 bp). 88.2% (1,980 reads) in M, 96.9% (436 reads) in M+C, 99.2% (9,654 reads) in G and 99.5% (2,328 reads) in G+C were classified into the domain Bacteria. Bacterial composition and diversity were compared at the same sequence reads (436 reads) for a fair comparison (Table 2 and 3).

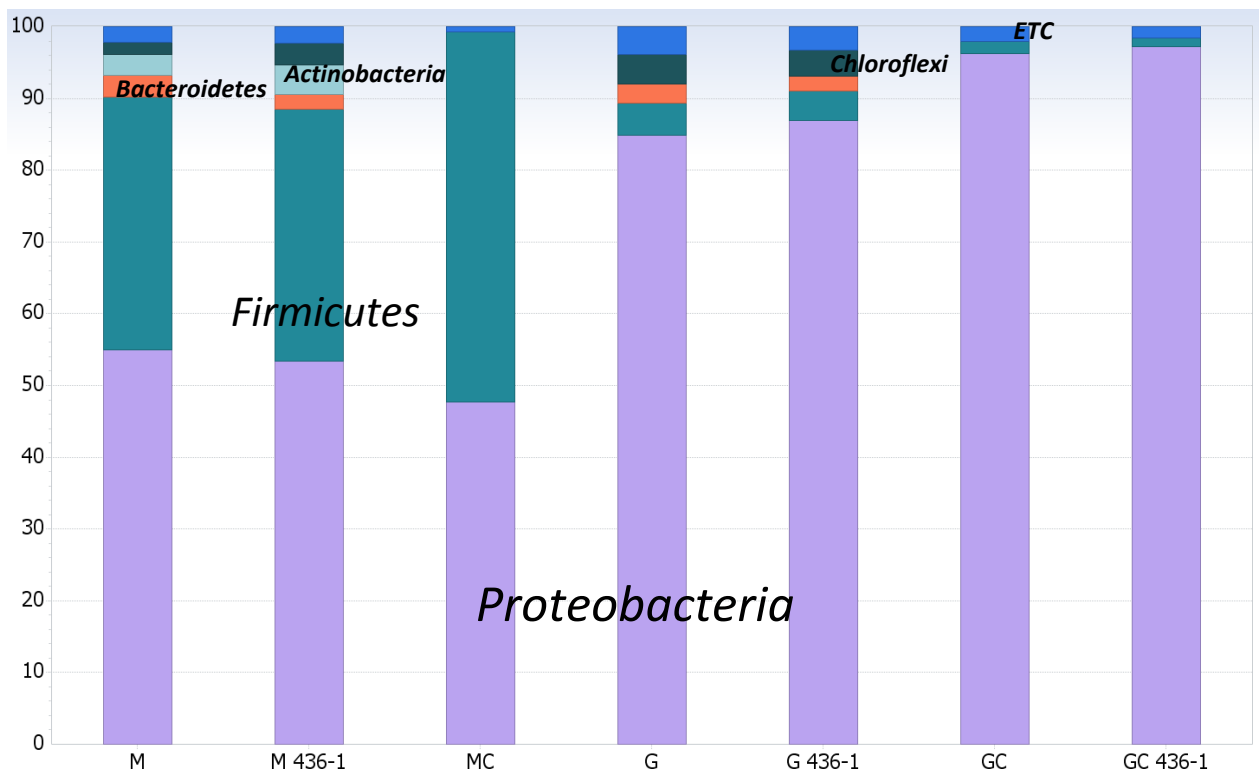


Figure 2. Phylum-level relative compositions of the full pyrosequenced bacterial communities and the average values of random subsets (436 reads)

Anode bacterial communities in a phylum level were distinctly different between the magnesium anodes and the graphite anodes (Fig. 2). The magnesium anodes were dominated by *Proteobacteria* (56.1% in M and 47.7% in M+C) and *Firmicutes* (35.1% in M and 51.6% in M+C), but the graphite anodes were dominated by *Proteobacteria* (85.6% in G and 96.3% in G+C). However, anode bacterial communities in a class level were very different among the four anodes. An anode bacterial community of M was most diverse and was comprised of *Deltaproteobacteria* (34.8%), *Bacilli* (18.8%), *Clostridia* (15.4%) and *Gammaproteobacteria* (11.2%), whereas an anode bacterial community of M+C was dominated by *Bacilli* (51.6%) and *Alphaproteobacteria* (47.2%). Anode bacterial communities of the graphite anode were dominated by *Deltaproteobacteria* (83.5% in G and 95.9% in G+C).

Although magnesium corrosion was a main process of power production in the magnesium-anode SMFCs, species-level anode bacterial communities were very different between M and M+C. Uncultured *Desulfuromusa* clone (16.4%), *Staphylococcus xylosus* (15.1%), *Desulfomicrobium baculatum* (9.8%), *Desulfobotulus alkaliphilus* (4.8%) and *Escherichia coli* (4.6%) were the five most dominant species in M, but *Afipia birgiae* (27.3%), *Bacillus subtilis* (22.7%), *Bradyrhizobium*

japonicum (11.2%), *Bacillus mojavensis* (10.8%) and *Bacillus siamensis* (9.2%) were the five most dominant species in M+C.

Table 3. Richness and diversity estimates of the sediment anode bacterial communities at 436 sequence reads

Sample	Reads	ACE ³	HCI ²	LCI ²	Chao ⁴	HCI ²	LCI ²	Jack ⁵	HCI ²	LCI ²
M	436	422	571	326	298	430	225	374	465	283
M+C	436	29	53	23	28	58	22	28	35	21
G	436	489	658	369	316	662	176	1,071	1,850	292
G+C	436	150	225	107	93	192	59	159	238	80
Sample	OTUs ¹	NpSh ⁶	Shannon ⁷	HCI ²	LCI ²	Simpson ⁸	HCI ²	LCI ²	Inverse Simpson ⁹	Cov. ¹⁰
M	133	4.14	3.73	3.89	3.57	6.21E-02	7.40E-02	5.02E-02	16.3	79.8%
M+C	21	1.64	1.57	1.70	1.45	3.20E-01	3.50E-01	2.91E-01	3.1	98.4%
G	79	3.42	3.18	3.32	3.05	7.58E-02	8.75E-02	6.40E-02	13.4	87.9%
G+C	42	2.33	2.16	2.30	2.01	2.28E-01	2.59E-01	1.96E-01	4.9	94.4%

1) Operational taxonomic units (OTUs) were defined at 97% sequence similarity
 2) 95% HCI-LCI is the range of each index at 95% confidence interval
 3) Abundance-based coverage estimator, ACE ; 4) Abundance-based estimator, Chao1
 5) Interpolated Jackknife richness estimate ; 6) Non-parametric estimate of the classical Shannon diversity index
 7) Shannon index of diversity ; 8) Simpson index of diversity (λ)
 9) Inverse Simpson index = $1/\lambda$; 10) Coverage as calculated by the method of Good

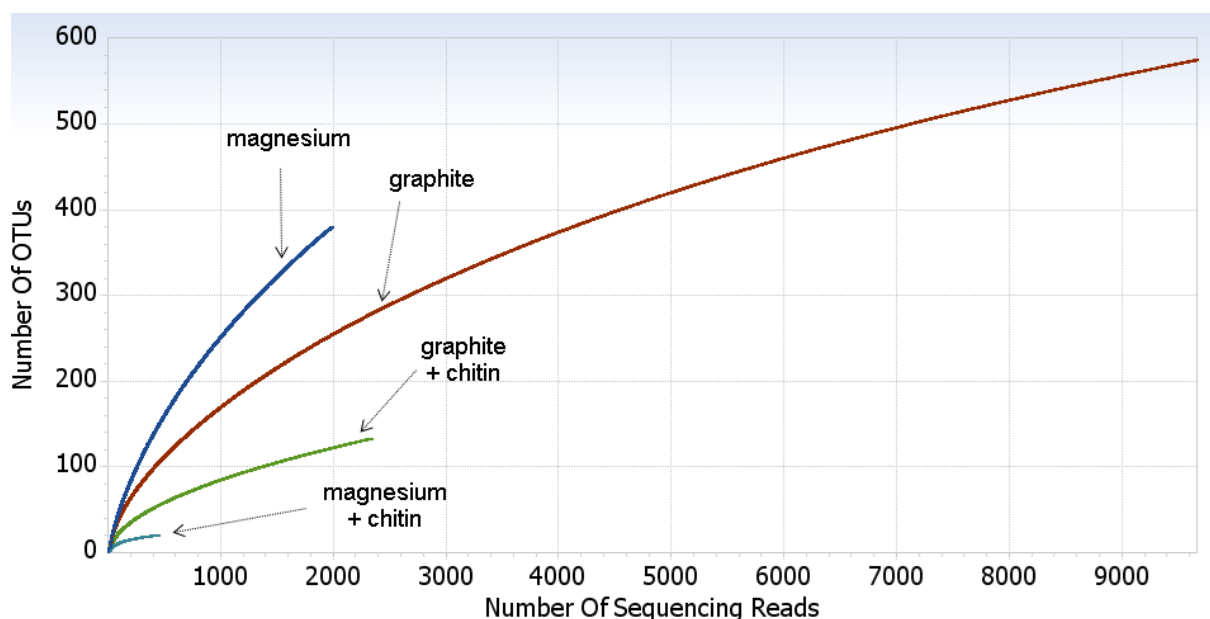


Figure 3. Rarefaction curves of pyrosequenced bacterial communities

Anode bacterial communities of the graphite anodes were dominated by a few species. Two uncultured *Deltaproteobacteria* clones (48.3% and 16.1%) and an uncultured *Desulfobulbaceae* cone (8.5%) were the three most dominant species in G, where most of species-level sequences were found to be uncultured. *Desulfuromonas acetoxidans* (76.9%). uncultured *Desulfuromonas* clone (13.5%) were the two most dominant species in an anode bacterial community of G+C. *Desulfuromonas acetoxidans* in G+C was likely to be a main species for bioelectricity production. In previous study, *D. acetoxidans* was also detected and isolated from a sediment MFC and the isolated strain successfully produced electricity in an MFC condition [21]. Anode bacterial communities of the magnesium anodes were diverse than the graphite anodes, and the supplemented chitin greatly influenced anode bacterial community compositions.

Anode bacterial communities of the chitin-absent anodes had larger richness estimates and diversity estimates than those of the chitin-supplemented anodes (Table 3). CD-HIT-based rarefaction curves show that anode bacterial community in M had the richest species diversity followed by G, G+C and M+C (Fig. 3). All the tested richness estimates (ACE, Chao, Jack) were highest in anode bacterial community of G, followed by M, G+C and M+C. The richness estimates of anode bacterial communities of the chitin-absent anodes (M and G) were one order of magnitude larger than those of the chitin-supplemented anodes (M+C and G+C). Because of the counterintuitive behavior of the Simpson index, the inverse Simpson index, which equals true diversity of order 2, were used in comparing diversity estimates [22, 23]. All the tested diversity estimates (NpSh, Shannon, Inverse Simpson) were highest in anode bacterial community of M, followed by G, G+C and M+C. The diversity estimates of anode bacterial communities of the chitin-absent anodes were also larger than those of the chitin-supplemented anodes. These results suggest that saturated carbon source, chitin, greatly simplified anode bacterial communities.

ACKNOWLEDGEMENTS

This work was supported by research grants (2012R1A2A4A01001539; 2013056833) from National Research Foundation of Korea (NRF).

References

1. C.E. Reimers, L.M. Tender, S. Fertig, W. Wang, *Environ Sci Technol*, 35 (2001) 192-195.
2. L.M. Tender, C.E. Reimers, H.A. Stecher, D.E. Holmes, D.R. Bond, D.A. Lowy, K. Pilobello, S.J. Fertig, D.R. Lovley, *Nat Biotech*, 20 (2002) 821-825.
3. D.A. Lowy, L.M. Tender, J.G. Zeikus, D.H. Park, D.R. Lovley, *Biosens Bioelectron*, 21 (2006) 2058-2063.
4. F. Rezaei, T.L. Richard, R.A. Brennan, B.E. Logan, *Environ Sci Technol*, 41 (2007) 4053-4058.
5. D.A. Lowy, L.M. Tender, *J Power Sources*, 185 (2008) 70-75.
6. K. Scott, I. Cotlarciuc, D. Hall, J. Lakeman, D. Browning, *J Appl Electrochem*, 38 (2008) 1313-1319.
7. M.H. Yoon, S.H. Jung, S.M. Lee, J.K. Yang, *J Korean Soc Water Sci and Technol*, 19 (2011) 11-20.
8. A. Shantaram, H. Beyenal, R.R.A. Veluchamy, Z. Lewandowski, *Environ Sci Technol*, 39 (2005) 5037-5042.

9. A. Rhoads, H. Beyenal, Z. Lewandowski, *Environ Sci Technol*, 39 (2005) 4666-4671.
10. D.E. Holmes, D.R. Bond, R.A. O'Neil, C.E. Reimers, L.R. Tender, D.R. Lovley, *Microb Ecol*, 48 (2004) 178-190.
11. S. Jung, J.M. Regan, *Appl Environ Microb*, 77 (2011) 564-571.
12. S. Jung, M.M. Mench, J.M. Regan, *Environ Sci Technol*, 45 (2011) 9069-9074.
13. B.E. Logan, J.M. Regan, *Trends Microbiol*, 14 (2006) 512-518.
14. S.P. Jung, *J Kor Soc Urban Environ* 13 (2013) 93-100.
15. S. Jung, *Int J Electrochem Sci*, 7 (2012) 11091-11100.
16. S. Cheng, H. Liu, B.E. Logan, *Electrochem Commun*, 8 (2006) 489-494.
17. J. Chun, J.-H. Lee, Y. Jung, M. Kim, S. Kim, B.K. Kim, Y.-W. Lim, *Int J Syst Evol Micr*, 57 (2007) 2259-2261.
18. L. Fu, B. Niu, Z. Zhu, S. Wu, W. Li, *Bioinformatics*, 28 (2012) 3150-3152.
19. P.D. Schloss, S.L. Westcott, T. Ryabin, J.R. Hall, M. Hartmann, E.B. Hollister, R.A. Lesniewski, B.B. Oakley, D.H. Parks, C.J. Robinson, J.W. Sahl, B. Stres, G.G. Thallinger, D.J. Van Horn, C.F. Weber, *Appl Environ Microb*, 75 (2009) 7537-7541.
20. B.E. Logan, *Microbial Fuel Cells*, Wiley & Sons, Inc., Hoboken, 2008.
21. D.R. Bond, D.E. Holmes, L.M. Tender, D.R. Lovley, *Science*, 295 (2002) 483-485.
22. L. Jost, *Oikos*, 113 (2006) 363-375.
23. M.O. Hill, *Ecology*, 54 (1973) 427-432.